

Bivariate Infinite Series Solution of Kepler's Equations

Daniele Tommasini

December 25, 2020

Abstract A class of bivariate infinite series solutions of the elliptic and hyperbolic Kepler equations is described, adding to the handful of 1-D series that have been found throughout the centuries. This result is based on the exact analytical computation of the partial derivatives of the eccentric anomaly with respect to the eccentricity e and mean anomaly M in a given base point (e_c, M_c) of the (e, M) plane. Explicit examples of such bivariate infinite series are provided, corresponding to different choices of (e_c, M_c) , and their convergence is studied. In particular, the polynomials that are obtained by truncating the infinite series up to the fifth degree reach high levels of accuracy in significantly large regions of the parameter space (e, M) .

Keywords analytical solutions · elliptic Kepler equation · hyperbolic Kepler equation

1 Introduction

In the Newtonian approximation, the time dependence of the relative position of two distant or spherically symmetric bodies that move in each other's gravitational field can be written with explicit analytical formulas involving a finite number of terms only when the eccentricity, e , is equal to 0 or 1, corresponding to circular and parabolic orbits, respectively [1]. For $0 < e < 1$ and for $e > 1$, such evolution can be obtained by solving for E one of the following two Kepler Equations (KEs) (see e.g. Chap. 4 of Ref. [1]),

$$M = f(e, E) = \begin{cases} E - e \sin E, & \text{for } e < 1 \\ e \sinh E - E, & \text{for } e > 1 \end{cases}, \quad (1)$$

D. Tommasini

Applied Physics Department, School of Aeronautic and Space Engineering, Universidade de Vigo

E-mail: daniele@uvigo.es

where M and E are measures of the epoch and the angular position called the mean and the eccentric anomaly, respectively (for convenience, the same symbols are used here for the elliptic and hyperbolic anomalies, even though they are defined in different ways).

A handful of infinite series solutions of Eqs. (1) have been found throughout the centuries (see Chap. 3 in Ref. [2]). The solution for $0 < e < 1$ has been written as an expansion in powers of e [3], or as an expansion in the basis functions $\sin(nM)$ with coefficients proportional to the values $J_n(e)$ of Bessel functions [4]. Levi-Civita [5,6] described a series in powers of the combination $z = \frac{e \exp(\sqrt{1-e^2})}{1+\sqrt{1-e^2}}$. Finally, Stumpff found an infinite series expansion in powers of M [7].

This article describes a class of solutions of KEs, Eqs. (1), in terms of bivariate infinite series in powers of both e and M ,

$$E = \sum_{k=0}^{\infty} \sum_{q=0}^{\infty} c_{k,q} (e - e_c)^k (M - M_c)^q, \quad (2)$$

with coefficients $c_{k,q}$ depending on the choice of the base values (e_c, M_c) . These solutions converge locally around (e_c, M_c) , and may be used to devise 2-D spline algorithms for the numerical computation of the eccentric anomaly E for every (e, M) , generalising the 1-D spline methods that have been described recently [8,9].

2 Methods

Let the unknown exact solution of Eq. (1) be

$$E = g(e, M). \quad (3)$$

If the analytical expression of the partial derivatives of $g(e, M)$ were known, a bivariate Taylor expansion could be written for any choice of base values $e_c, E_c, M_c = f(e_c, E_c)$, so that Eq. (2) would be demonstrated with the coefficients given by

$$c_{k,q} = \frac{1}{k!q!} \left[\frac{\partial^{k+q} g}{\partial e^k \partial M^q} (e_c, M_c) \right]. \quad (4)$$

In order to obtain such derivatives, we notice that the definitions in Eqs. (1) and (3) imply the identity,

$$E = g(e, f(e, E)). \quad (5)$$

In this expression, e and E are considered as the independent variables. Therefore, by taking the differential, we obtain,

$$dE = \frac{\partial g}{\partial e}(e, f(e, E)) de + \frac{\partial g}{\partial M}(e, f(e, E)) \left[\frac{\partial f}{\partial e}(e, E) de + \frac{\partial f}{\partial E}(e, E) dE \right]. \quad (6)$$

Since e and E are independent, the coefficients of dE and de must cancel separately. This condition can be used to obtain the partial derivatives of g . Taking also into account Eqs. (1) and (3), the cancellation of the coefficient of dE implies,

$$\frac{\partial g}{\partial M}(e, M) = \frac{1}{\frac{\partial f}{\partial E}(e, g(e, M))} \equiv \frac{\lambda}{1 - eC}, \quad (7)$$

where we have defined the parameter λ and the functions C such that $\lambda = 1$ and $C = \cos g(e, M)$, for $e < 1$, or $\lambda = -1$ and $C = \cosh g(e, M)$, for $e > 1$. As it could be expected, Eq. (7) coincides with the usual rule for the derivative of the inverse function when e is considered to be a fixed parameter. The cancellation of the coefficient of de in Eq. (6) implies,

$$\frac{\partial g}{\partial e}(e, M) = -\frac{\partial g}{\partial M}(e, M) \frac{\partial f}{\partial e}(e, g(e, M)) \equiv \frac{S}{1 - eC}, \quad (8)$$

with S defined as $S = \sin g(e, M)$, for $e < 1$, or $S = \sinh g(e, M)$, for $e > 1$.

Eqs. (7) and (8), taken together with Eqs. (1) and (3), can be used for the iterative computation of all the higher order derivatives entering Eq. (2) for $e \neq 1$. The calculations can be simplified by expressing all the derivatives in terms of only λ , S , and C , and using the following identities, which can be derived from the definitions of S and C and Eqs. (7) and (8),

$$\frac{\partial S}{\partial e}(e, M) = \frac{C S}{1 - eC}, \quad \frac{\partial S}{\partial M}(e, M) = \frac{\lambda C}{1 - eC}, \quad (9)$$

$$\frac{\partial C}{\partial e}(e, M) = -\frac{\lambda S^2}{1 - eC}, \quad \frac{\partial C}{\partial M}(e, M) = -\frac{S}{1 - eC}. \quad (10)$$

The second order derivatives can then be obtained by applying the operators $\frac{\partial}{\partial e}$ and $\frac{\partial}{\partial M}$ and the rules of Eqs. (9) and (10) to the first order derivatives given in Eqs. (7) and (8). The result is,

$$\frac{\partial^2 g}{\partial e^2}(e, M) = \frac{2 C S}{(1 - eC)^2} - \frac{\lambda e S^3}{(1 - eC)^3}, \quad (11)$$

$$\frac{\partial^2 g}{\partial M^2}(e, M) = -\frac{\lambda e S}{(1 - eC)^3}, \quad (12)$$

$$\frac{\partial^2 g}{\partial e \partial M}(e, M) = \frac{\lambda C}{(1 - eC)^2} - \frac{e S^2}{(1 - eC)^3}. \quad (13)$$

Similarly, the third order derivatives can be obtained by applying the operators $\frac{\partial}{\partial e}$ and $\frac{\partial}{\partial M}$ and the rules of Eqs. (9) and (10) to the second order derivatives, Eqs. (11), (12), and (13). The result is,

$$\frac{\partial^3 g}{\partial e^3}(e, M) = \frac{6 C^2 S - 3 \lambda S^3}{(1 - eC)^3} - \frac{10 \lambda e C S^3}{(1 - eC)^4} + \frac{3 e^2 S^5}{(1 - eC)^5}, \quad (14)$$

$$\frac{\partial^3 g}{\partial M^3}(e, M) = -\frac{e C}{(1 - eC)^4} + \frac{3 \lambda e^2 S^2}{(1 - eC)^5}, \quad (15)$$

$$\frac{\partial^3 g}{\partial e^2 \partial M}(e, M) = \frac{2 \lambda C^2 - 2 S^2}{(1 - e C)^3} - \frac{7 e C S^2}{(1 - e C)^4} + \frac{3 \lambda e^2 S^4}{(1 - e C)^5}, \quad (16)$$

$$\frac{\partial^3 g}{\partial e \partial M^2}(e, M) = -\frac{\lambda S}{(1 - e C)^3} - \frac{4 \lambda e C S}{(1 - e C)^4} + \frac{3 e^2 S^3}{(1 - e C)^5}. \quad (17)$$

All the higher order derivatives can be obtained by iterating this procedure. These expressions are exact, but they depend on the unknown function g through S and C . Nevertheless, taken together with Eq. (3), they can be used to compute 2-D Taylor series solutions of KEs. This can be done by choosing a pair of base values, e_c and E_c , corresponding to $M_c = f(e_c, E_c)$. The values of the coefficients entering Eqs. (4) and (2) can then be computed by substituting $\lambda = 1$, $S = \sin E_c$, $C = \cos E_c$, for $e_c < 1$, or $\lambda = -1$, $S = \sinh E_c$, $C = \cosh E_c$, for $e_c > 1$, in the expressions for the derivatives of g , and by defining the zeroth order term $\frac{\partial^0 g}{\partial e^0 \partial M^0}(e_c, M_c) = g(e_c, M_c) = E_c$. This procedure can be used to build a class of bivariate infinite series solutions of the elliptic and hyperbolic KEs, one for any given choice of base values. Three explicit examples will be given in Sec. 3.

The determination of the radius of convergence for the univariate series has been a formidable mathematical problem (see Chap. 6 of Ref. [2]). Although the rigorous generalisation of such analyses to the bivariate series of Eqs. (2) and (4) surpasses the scope of this letter, a practical criterion for estimating the region of convergence will still be given in Sec. 3.

3 Examples, discussion and results

In this section, three examples of bivariate infinite series solutions of KEs are given. They have been obtained from Eqs. (2) and (4) by applying the methods discussed in Sec. 2 for the computation of the derivatives of g , for three different choices of the base values (e_c, M_c) . All the non-vanishing terms up to fifth order are shown explicitly. Since $g(e, -M) = -g(e, M)$, it is sufficient to solve KEs only for positive values of M . Moreover, for $e < 1$ the M domain can be reduced to the interval $0 \leq M \leq \pi$, and then the solution for every M can be obtained by using the periodicity of f and g .

In all cases, it is convenient to define approximate solutions S_n obtained by truncating the infinite series of Eq. (2) keeping only the terms with $k + q \leq n$, so that

$$S_n(e, M) = \sum_{k=0}^n \sum_{q=0}^{n-k} c_{k,q} (e - e_c)^k (M - M_c)^q, \quad (18)$$

with coefficients given by Eq. (4). The errors \mathcal{E}_n of the approximate solutions S_n can then be evaluated in a self consistent way,

$$\mathcal{E}_n(e, M) = |S_n(e, M) - S_n(e, f(e, S_n(e, M)))|. \quad (19)$$

From a practical point of view, the convergence of the infinite series for certain values of (e, M) means that $\mathcal{E}_n(e, M)$ should tend to decrease for increasing n . This idea is used for obtaining an estimate of the region of convergence in the (e, M) parameter space by comparing the average errors for lower and higher values of n with the following rule of thumb,

$$\mathcal{E}_1(e, M) + \mathcal{E}_2(e, M) + \mathcal{E}_3(e, M) > \frac{3}{2} [\mathcal{E}_4(e, M) + \mathcal{E}_5(e, M)]. \quad (20)$$

3.1 Bivariate infinite series solution of the elliptic Kepler equation around $e_c = 0, M_c = 0$

Choosing $e_c = 0, E_c = 0$, so that $M_c = 0$ rad, $\lambda_c = 1, S_c = 0, C_c = 1$, the series of Eqs. (2) and (4) becomes,

$$E = M + eM + e^2M + e^3M - \frac{e}{6}M^3 + e^4M - \frac{2}{3}e^2M^3 + \dots \quad (21)$$

Fig. 1 shows the variation of the errors $\mathcal{E}_n(e, M)$, Eq. (19), computed along the line $M = \pi e$, when the bivariate polynomials S_n of Eqs. (18) are obtained by truncating Eq. (21) to degree n . Along this line, the error \mathcal{E}_5 is at the level of arithmetic double precision ($\epsilon_{\text{double}} = 2.23 \times 10^{-16}$) for $e = \frac{M}{\pi} \lesssim 0.0013$. For almost all values of $e \lesssim 0.6$ the error decreases as n increases, as expected for a convergent series. Below this value, inversions in the order of the \mathcal{E}_n s only occur around $e \sim 0.3$ and $e \sim 0.4$, when the second order and the first order approximations, respectively, become smaller than higher order ones. For $e \gtrsim 0.8$, the inversions become more evident and cannot be justified any longer with oscillatory terms in f and g . These considerations hint at the conclusion that in this specific direction the limit for convergence should be somewhere in between $e \sim 0.6$ and $e \sim 0.8$. A more precise, though still approximate, criterion of convergence may be obtained with the rule of thumb of Eq. (20). In the case of the $M = \pi e$ line, this rule gives the values $e < 0.72$ (or $M < 2.2$ rad), in agreement with the conclusion obtained from the qualitative analysis of Fig. 1.

Fig. 2 shows the contour levels in the (e, M) plane of the error \mathcal{E}_5 affecting the fifth degree polynomial approximation, S_5 , as given by Eq. (21). The limit $e < 0.6627434193$ for the convergence of Lagrange's univariate series (see page 26 of Ref. [2]) is represented by the vertical dashed magenta line. The continuous black curve marks the boundary of the region of convergence of the bivariate series of Eq. (21), as estimated with Eq. (20). The error \mathcal{E}_5 is kept below $\sim 10^{-4}$ rad for $e \lesssim 0.5$ and $M \lesssim \pi/2$, and is reduced to the level $\sim 10^{-13}$ rad for $e \sim 0.01$ and $M \sim \pi/1000$. Moreover, the fifth order approximation reaches machine precision ϵ_{double} in an entire neighbourhood of size $\Delta e \sim 2 \times 10^{-3}, \Delta M \sim 3 \times 10^{-3}$ rad around the point (e_c, M_c) .

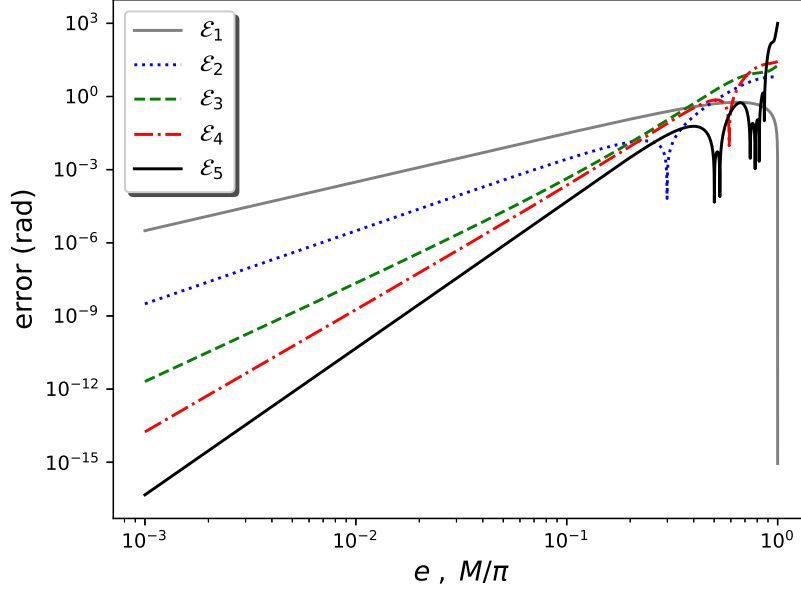


Fig. 1 Errors $\mathcal{E}_n(e, M)$ affecting the approximate polynomial solutions $S_n(e, M)$ of KE, as a function of the eccentricity e (in logarithmic scale). The S_n are obtained by truncating the infinite series of Eq. (21) up to degree n , for $n = 1, \dots, 5$, and the plotted errors have been computed along the line $M = \pi e$ of the (e, M) plane.

3.2 Bivariate infinite series solution of the elliptic Kepler equation around $e_c = \frac{1}{2}$, $M_c = \frac{\pi-1}{2}$

Choosing $e_c = \frac{1}{2}$, $E_c = \frac{\pi}{2}$, so that $M_c = \frac{\pi-1}{2}$, $\lambda_c = 1$, $S_c = 1$, $C_c = 0$, and defining $\delta = e - e_c = e - \frac{1}{2}$ and $\Delta = M - M_c = M - \frac{\pi-1}{2}$, the series of Eqs. (2) and (4) becomes,

$$\begin{aligned}
 E = & \frac{\pi}{2} + \Delta + \delta - \frac{\delta^2 + 2\delta\Delta + \Delta^2}{4} + \frac{-3\delta^3 - 5\delta^2\Delta - \delta\Delta^2 + \Delta^3}{8} + \\
 & + \frac{85\delta^4 + 244\delta^3\Delta + 222\delta^2\Delta^2 + 52\delta\Delta^3 - 11\Delta^4}{192} + \\
 & + \frac{37\delta^5 - 35\delta^4\Delta - 318\delta^3\Delta^2 - 374\delta^2\Delta^3 - 119\delta\Delta^4 + 9\Delta^5}{384} + \dots
 \end{aligned} \tag{22}$$

The errors $\mathcal{E}_n(e, M)$ shown in Fig. 3 for five polynomials S_n , obtained by truncating Eq. (22) to degree n , have been computed along the two lines connecting the opposite points $(0, 0)$ and $(1, \pi)$ of the (e, M) domain with the mid point $(e_c, M_c) = (\frac{1}{2}, \frac{\pi-1}{2})$. For most values of $e \lesssim 0.6$ the errors tend

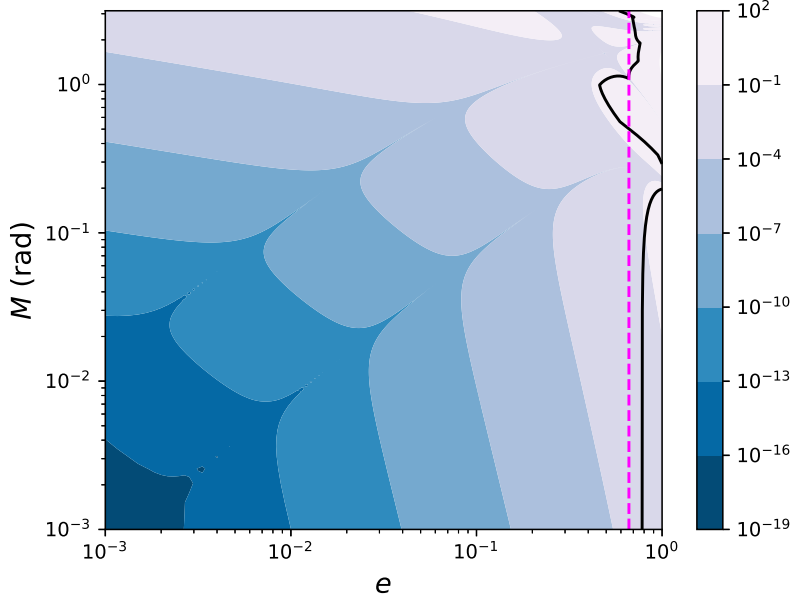


Fig. 2 Contour levels of the error $\mathcal{E}_5(e, M)$ affecting the fifth degree polynomial approximation, Eq. (21), as a function of the eccentricity e and the mean anomaly M (both in logarithmic scales). The continuous black curve marks the boundary of the region of convergence for the bivariate series of Eq. (21), as estimated with Eq. (20). The vertical dashed magenta line represents the limit of the region of convergence for Lagrange's univariate series.

to decrease as n increases, though the inversions become more evident as e approaches 1. In this case, the rule of thumb of Eq. (20) gives the values $e < 0.87$ (or $M < 2.7$ rad) along this line.

Fig. 4 shows the contour levels in the (e, M) plane of the error \mathcal{E}_5 affecting the fifth degree polynomial approximation, S_5 , as given by Eq. (22). The continuous black curve marks the boundary of the region of convergence, as estimated with Eq. (20). It can be seen that the Taylor series based in the mid point $(\frac{1}{2}, \frac{\pi-1}{2})$ converges for most values of (e, M) , although even in this case there are two small regions in which it is expected to diverge. Moreover, the fifth degree polynomial reaches machine precision ϵ_{double} in an elongated neighbourhood of the point $(\frac{1}{2}, \frac{\pi-1}{2})$ along a diagonal line crossing the entire e domain from $(e = 0, M = 1.57 \text{ rad})$ to $(e \simeq 1, M = 0.56 \text{ rad})$, with transverse size (along the M direction) ranging from $\sim 3 \times 10^{-3}$ rad close to the endpoints, to $\sim 10^{-2}$ rad around the centre (e_c, M_c) .

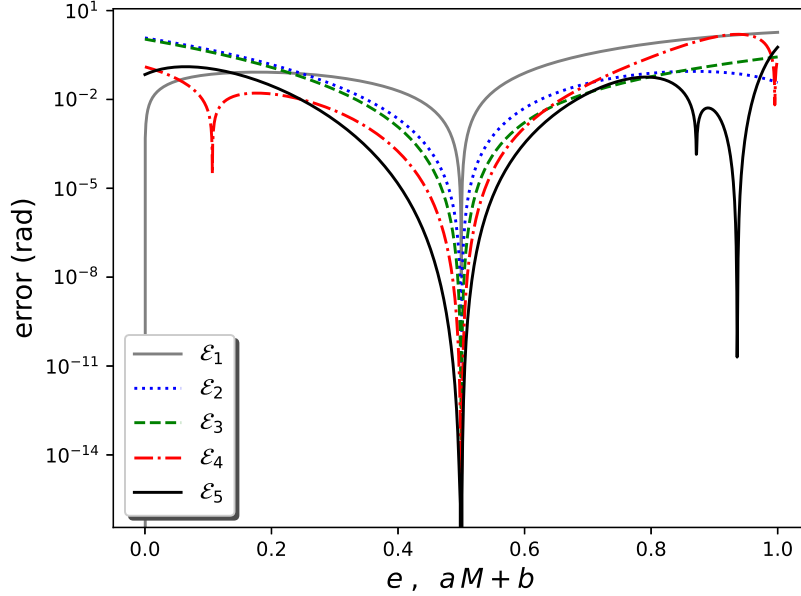


Fig. 3 Errors $\mathcal{E}_n(e, M)$ for the approximate polynomial solutions $S_n(e, M)$ of KE, obtained by truncating the infinite series of Eq. (22) up to degree n , for $n = 1, \dots, 5$. The errors have been computed along the two lines connecting the points $(0, 0)$, $(\frac{1}{2}, \frac{\pi-1}{2})$, and $(1, \pi)$ of the (e, M) plane, so that $a = \frac{1}{\pi-1}$ and $b = 0$ for $e < 0.5$, and $a = b = \frac{1}{\pi+1}$ for $e > 0.5$. (Notice that here only the vertical axis is logarithmic, while the horizontal axis is chosen to be linear.)

3.3 Bivariate infinite series solution of the hyperbolic Kepler equation around $e_c = 2$, $M_c = 0$

Choosing $e_c = 2$, $E_c = 0$, so that $M_c = 0$, $\lambda_c = -1$, $S_c = 0$, $C_c = 1$, defining $\delta = e - e_c = e - 2$, the series of Eqs. (2) and (4) becomes,

$$E = M - M\delta + M\delta^2 - \frac{M^3}{3} - M\delta^3 + \frac{7M^3\delta}{6} + M\delta^4 - \frac{8M^3\delta^2}{3} + \frac{19M^5}{60} + \dots, \quad (23)$$

where now E and M indicate the (dimensionless) hyperbolic anomalies.

Fig. 5 shows the variation of the errors $\mathcal{E}_n(e, M)$ computed along the line $M = e - 2$, for $0 < M \leq 1$, when the bivariate polynomials S_n of Eqs. (18) are obtained by truncating Eq. (23) to degree n . Along this line, the error \mathcal{E}_5 reaches machine precision ϵ_{double} for $e - 2 = M \lesssim 0.002$. It can be seen that the inversions in the order of the errors \mathcal{E}_n become more and more important for $e - 2 \gtrsim 0.8$, in agreement with the estimate $e < 2.8$ (corresponding to $M < 0.8$) obtained by applying the condition of convergence Eq. (20) to the direction of the $M = e - 2$ line.

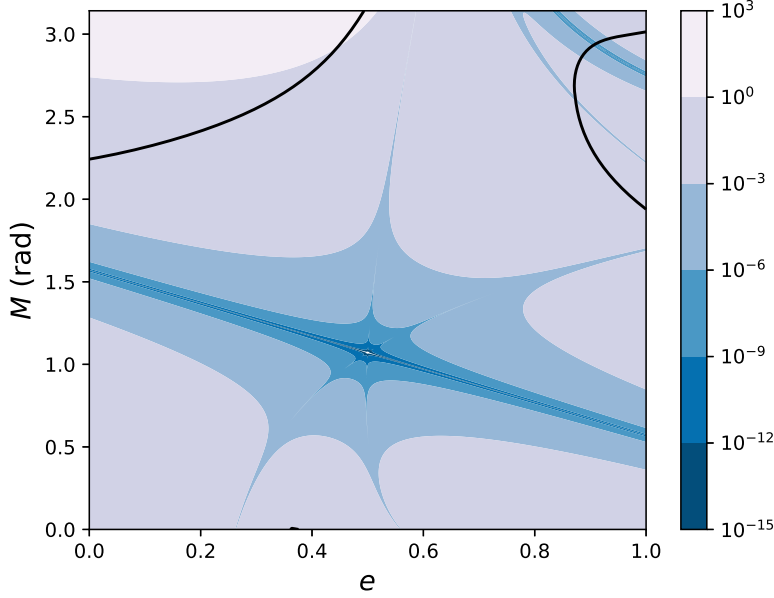


Fig. 4 Contour levels of the error \mathcal{E}_5 affecting the fifth degree polynomial approximation of Eq. (22), as a function of the eccentricity e and the mean anomaly M . The continuous black curve marks the boundary of the region of convergence, as estimated with Eq. (20). (Notice that here the axes for e and M are linear.)

For the hyperbolic motion, the values of e and M can vary in infinite ranges, $1 < e < \infty$, $0 < M < \infty$ (due to the symmetry for $M \rightarrow -M$). In Fig. 6, the contour levels in the (e, M) plane of the error \mathcal{E}_5 for the solution (23) have been drawn in the region $e \leq 4$, $M \leq 2$. This region has been chosen in such a way that the plot contains the continuous black curve marking the boundary of the region of convergence, as estimated with Eq. (20). Moreover, the fifth degree polynomial reaches machine precision ϵ_{double} in an entire neighbourhood of size $\Delta e \sim 8 \times 10^{-3}$, $\Delta M \sim 2 \times 10^{-3}$, around the point (e_c, M_c) .

4 Conclusions

I have described a novel analytical procedure for the exact computation of all the partial derivatives of the elliptic and hyperbolic eccentric anomalies with respect to both the eccentricity e and the mean anomaly M . Although such derivatives depend implicitly on the solution of KE, they can be computed explicitly by choosing a couple of base values e_c and E_c for the eccentricity and the eccentric anomaly, so that the corresponding value M_c of the mean anomaly can be obtained without solving KE. For any such choice of (e_c, M_c) , an infinite Taylor series expansion in both M and e can then be written,

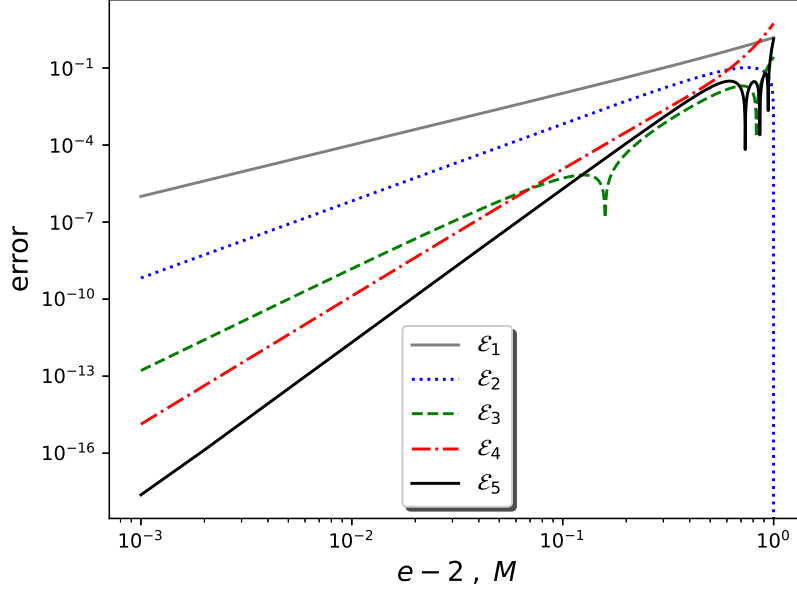


Fig. 5 Errors $\mathcal{E}_n(e, M)$ for the approximate polynomial solutions $S_n(e, M)$ of the hyperbolic KE, obtained by truncating the infinite series of Eq. (23), as functions of $e-2$ (in logarithmic scale). The errors have been computed along the line $M = e - 2$.

which is expected to converge in a suitable neighbourhood of (e_c, M_c) . A rule of thumb for estimating the actual size of the region of convergence has also been given.

Three explicit examples of such series have then been provided, two for the elliptic and one for the hyperbolic KE. Each of them, for fixed base point, turns out to converge in large parts of the (e, M) plane. For (e, M) close to (e_c, M_c) within a range $\Delta e \sim \Delta M/\pi = \mathcal{O}(10^{-3})$, the polynomial obtained by truncating the infinite series up to the fifth degree reaches an accuracy at the level of machine double precision. More far away from (e_c, M_c) , but still within the region of convergence, higher order terms should be introduced to maintain such an accuracy.

Since these new solutions converge locally around (e_c, M_c) , a suitable set of them, centred around different (e_c, M_c) and truncated up to a certain degree, may be used to design an algorithm for the numerical computation of the function $E(e, M)$ for every value of (e, M) . The resulting polynomials would form a 2-D spline, generalising the 1-D spline that has been proposed in Refs. [8, 9] for solving KE for every M when e is fixed.

Acknowledgements I thank David N. Olivieri for discussions. This work was supported by grants ED431B 2018/57 from Xunta de Galicia, Consellería de Educación, Universidade

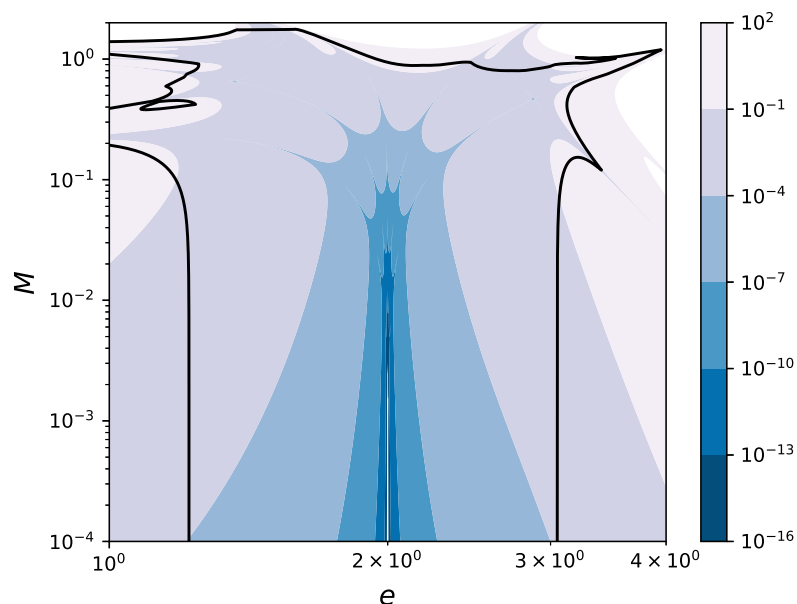


Fig. 6 Contour levels of the error \mathcal{E}_5 affecting the fifth degree polynomial approximation of Eq. (23), as a function of the eccentricity e and the mean anomaly M (both in logarithmic scale). The continuous black curve marks the boundary of the region of convergence, as estimated with Eq. (20).

e Formacion Profesional, and FIS2017-83762-P from Ministerio de Economia, Industria y Competitividad, Spain.

References

1. A.E. Roy, *Orbital Motion*, 4th edn. (Institute of Physics Publishing, Bristol and Philadelphia, 2005)
2. P. Colwell, *Solving Kepler's Equation Over Three Centuries* (Willmann-Bell Inc., Richmond, VA, 1993)
3. J. Lagrange, *Memoires de l'Academie Royale des Sciences* (Berlin) **25**, 204 (1771)
4. F. Bessel, *Monatliche Correspondenz zur Beforderung der Erd-und Himmels-Kunde herausgegeben von Freiherrn von Zach* **12**, 197 (1805)
5. T. Levi-Civita, *Astronomische Nachrichten* **164**, 313 (1904)
6. T. Levi-Civita, *Rendiconti della Reale Accademia dei Lincei, Classe di scienze fisiche, matematiche e naturali E* **13**, 260 (1904)
7. K. Stumpff, National Aeronautics and Space Administration **Technical Note D-4460** (1968)
8. D. Tommasini, D.N. Olivieri, *Applied Mathematics and Computation* **364**, 124677 (2020). DOI <https://doi.org/10.1016/j.amc.2019.124677>
9. D. Tommasini, D.N. Olivieri, *Mathematics* **8(11)**, 2017 (2020). DOI 10.3390/math8112017